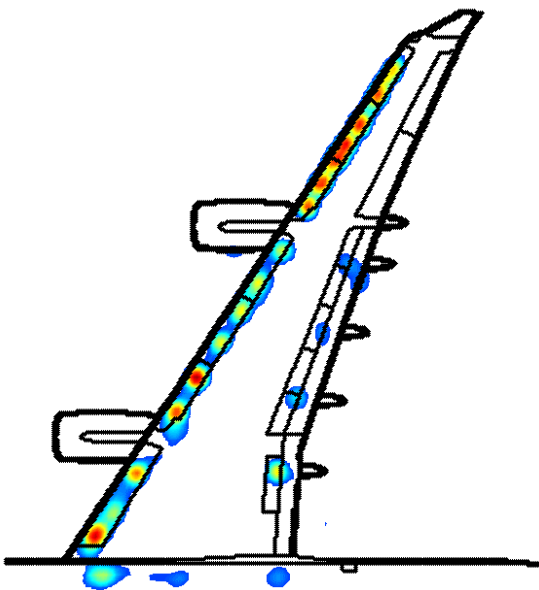




Executive summary

CLEAN based on spatial source coherence

AIAA Paper 2007-3436



Problem area

Since a few years, deconvolution is an extensively studied topic of phased array beamforming with wind tunnel microphone arrays. Most deconvolution methods aim at identifying Point Spread Functions (PSF's) in source plots. PSF's are theoretical beam patterns obtained by applying Conventional Beamforming using synthetical microphone data of monopole point sources. The objective of deconvolution methods is the replacement of these PSF's by single points, or beams with narrow widths. The deconvolution method DAMAS, launched in 2004 by Brooks and Humphreys, has

become a standard tool. This method starts with incoherent PSF's of unknown strengths at each point of the scan grid. The unknown strengths are solved by an iterative procedure, where stability is guaranteed by a positivity constraint.

A possible disadvantage of deconvolution methods is the assumption that source plots are built up by PSF's. Actual beam patterns of measured noise sources may not be identical to the synthetically obtained PSF's. For example, actual sources may have a spatial extent rather than being concentrated in a point.

Report no.

NLR-TP-2007-345

Author(s)

P. Sijtsma

Report classification

UNCLASSIFIED

Date

December 2007

Knowledge area(s)

Aeroacoustic & Experimental
Aerodynamics

Descriptor(s)

Wind tunnels
Deconvolution
Microphone arrays

Furthermore, actual sources do not need to have uniform directivity, like monopole sources. In such cases, deconvolution methods may fall short.

Description of work

To overcome the disadvantages of a PSF-based method, a new deconvolution method is described here. This new method takes advantage of the fact that sources in source plots are spatially coherent with their side lobes. Beam patterns of individual noise sources are determined by analyzing the measured spatial coherence, thus avoiding the use of synthetic PSF's. The new method is called "CLEAN based on Source Coherence" or, briefly, "CLEAN-SC." It is an alternative version of the classical CLEAN method used in Astronomy, which iteratively removes PSF's of peak sources from a "dirty map". Essentially, CLEAN-SC iteratively removes the part of the source plot which is spatially coherent with the peak source. A feature of CLEAN-SC is its ability to extract absolute sound power levels from the source plots. The merits of CLEAN-SC were demonstrated using array measurements of airframe noise on a scale model of the Airbus A340 in the 8×6 m² closed test section of DNW-LLF.

Results and conclusions

It was found that CLEAN-SC is a very effective tool to remove dominant sources from source plots, thereby unmasking secondary sources. Like other deconvolution

algorithms, significant improvements in spatial resolution were found. Moreover, CLEAN-SC is able to extract absolute values of source components from the source plots. Summed results of these source powers agree very well with results of the conventional Source Power Integration technique. The processing time of CLEAN-SC is relatively short: about twice as long as for Conventional Beamforming.

Applicability

CLEAN-SC is very suitable for processing microphone array data from closed wind tunnel test sections.



NLR-TP-2007-345

CLEAN based on spatial source coherence

AIAA Paper 2007-3436

P. Sijtsma

This report is based on a presentation held at the 13th AIAA/CEAS Aeroacoustics Conference, Rome, 21-23 May, 2007.

The contents of this report may be cited on condition that full credit is given to NLR and the author.

This publication has been refereed by the Advisory Committee AEROSPACE VEHICLES.

Customer	German-Dutch Wind Tunnels DNW
Contract number	15.0003
Owner	National Aerospace Laboratory NLR
Division NLR	Aerospace Vehicles
Distribution	Unlimited
Classification of title	Unclassified
	December 2007

Approved by:

Author	Reviewer	Managing department
<i>PS 14-1-08</i>	<i>SO 14/1/08</i>	<i>[Signature] 17/1/08</i>

Contents

CLEAN based on spatial source coherence	3
ABSTRACT	3
NOMENCLATURE	3
1 Introduction	4
2 Theory	5
2.1 Conventional Beamforming	5
2.2 Point Spread Functions	6
2.3 Deconvolution using CLEAN-PSF	6
2.4 Deconvolution using CLEAN-SC	8
2.5 Determination of absolute source contributions using CLEAN-SC	10
3 Application to wind tunnel measurements	10
3.1 Typical results	10
3.2 Removal of dominant sources	15
4 Remarks about CLEAN-SC	18
4.1 Processing speed	18
4.2 Sources outside the scan area	18
4.3 Reflected sources	19
4.4 Closely spaced sources	19
4.5 Noise	19
4.6 CLEAN-SC using full CSM	19
5 Conclusion	20
Acknowledgment	20
References	20

CLEAN based on spatial source coherence

Pieter Sijtsma

*Senior Scientist, National Aerospace Laboratory NLR
P.O. Box 153, 8300 AD, Emmeloord, The Netherlands
sijtsma@nlr.nl*

ABSTRACT

To obtain higher resolution acoustic source plots from microphone array measurements, deconvolution techniques are becoming increasingly popular. Deconvolution algorithms aim at identifying Point Spread Functions (PSF) in source plots, and may therefore fall short when actual beam patterns of measured noise sources are not similar to synthetically obtained PSF's. To overcome this, a new version of the classical deconvolution method CLEAN is proposed here: CLEAN-SC. By this new method, which is based on spatial source coherence, side lobes can be removed of actually measured beam patterns. Essentially, CLEAN-SC iteratively removes the part of the source plot which is spatially coherent with the peak source. A feature of CLEAN-SC is its ability to extract absolute sound power levels from the source plots. The merits of CLEAN-SC were demonstrated using array measurements of airframe noise on a scale model of the Airbus A340 in the 8×6 m² closed test section of DNW-LLF.

NOMENCLATURE

CB	Conventional Beamforming
CLEAN-PSF	CLEAN based on PSF's
CLEAN-SC	CLEAN based on Source Coherence
CSM	Cross-Spectral Matrix
PC	Principal Component
PSF	Point Spread Function
SPI	Source Power Integration
A	source power
B_{jk}	source cross-power
C	CSM
\bar{C}	trimmed CSM (diagonal removed)
$D^{(i)}$	degraded CSM (source components removed)
F	cost function

$\mathbf{G}^{(i)}$	CSM induced by peak source
\mathbf{g}	steering vector
\mathbf{H}	matrix defined by Eqn (24)
\mathbf{h}	source component in $\bar{\mathbf{C}}$
I	number of iterations
i	iteration
j	scan point index
k	scan point index
m	microphone index
N	number of microphones
n	microphone index
$P_j^{(i)}$	degraded source powers (source components removed)
$Q_j^{(i)}$	synthetical source powers forming clean beam
S	subset of all possible (m,n) -combinations
\mathbf{w}	weight vector
$\gamma_{j,\max}^{2(i)}$	spatial source coherence
Φ	normalized clean beam
φ	loop gain
$\vec{\xi}$	point on scan grid

1 Introduction

Since a few years, deconvolution is an extensively studied topic of phased array beamforming in aeroacoustic measurements¹⁻⁶. An overview of deconvolution methods is given by Ehrenfried and Koop⁷. Deconvolution methods aim at identifying Point Spread Functions (PSF) in source plots, and replacing them by single points, or beams with narrow widths. The deconvolution method DAMAS, launched in 2004 by Brooks and Humphreys², has become a standard tool. This method starts with incoherent PSF's of unknown strengths at each point of the scan grid. The unknown strengths are solved by an iterative procedure, where stability is guaranteed by a positivity constraint. In 2006, DAMAS was extended to include spatial source coherence⁵.

A disadvantage of most deconvolution methods is the assumption that source plots are built up by PSF's. These are theoretical beam patterns (main lobe + side lobes) obtained by applying Conventional Beamforming (CB) using synthetical microphone data of monopole point sources. However, actual beam patterns of measured noise sources may not be identical to the synthetically obtained PSF's. For example, actual sources may have a spatial extent rather than being concentrated in a point. Furthermore, actual sources do not need to have uniform directivity, like monopole sources. In such cases, deconvolution methods may fall short.

To overcome the disadvantages of a PSF-based method, a new deconvolution method is proposed here, which is based on spatial source coherence⁸. This new method takes advantage of the fact that main lobes are spatially coherent with their side lobes, as they originate from the same physical source. Beam patterns of individual noise sources are determined by analyzing the measured spatial coherence, thus avoiding the use of synthetical PSF's. The new method is called "CLEAN based on Source Coherence" or, briefly, "CLEAN-SC." It is an alternative version of the classical CLEAN⁹ method used in Astronomy, which iteratively removes PSF's of peak sources from a "dirty map".

In Section 2 of this article the theory behind CLEAN-SC is treated. In Section 3 applications to airframe noise measurements on a scale model of the Airbus A340 are discussed. In Section 4 some remarks about CLEAN-SC are made, and the conclusions are summarized in Section 5.

2 Theory

2.1 Conventional Beamforming

The most straightforward way to process phased array data is the CB technique. This is a frequency-domain method, in which powers A of sources in points $\vec{\xi}$ in a scan area are determined as follows. Let N be the number of microphones, and \mathbf{C} the measured $N \times N$ cross-spectral matrix (CSM). Further, let \mathbf{g} be the N -dimensional steering vector, which consists of microphone pressure amplitudes induced by a unit monopole point source in $\vec{\xi}$. If S is a subset of all possible (m,n) -combinations, where m and n are microphone indices, then the source power A can be obtained through minimization of

$$F = \sum_{(m,n) \in S} |C_{mn} - A g_m g_n^*|^2, \quad (1)$$

where the asterisk means complex conjugation. The solution is

$$A = \sum_{(m,n) \in S} g_m^* C_{mn} g_n / \sum_{(m,n) \in S} |g_m|^2 |g_n|^2. \quad (2)$$

In wind tunnel measurements S usually contains all (m,n) -combinations with $m \neq n$. This means that the diagonal is removed from the CSM. Introducing the trimmed CSM $\bar{\mathbf{C}}$ by

$$\bar{C}_{mn} = \begin{cases} C_{mn}, & \text{for } (m,n) \in S, \\ 0, & \text{for } (m,n) \notin S, \end{cases} \quad (3)$$

and the weight vector \mathbf{w} by

$$\mathbf{w} = \mathbf{g} / \left(\sum_{(m,n) \in S} |\mathbf{g}_m|^2 |\mathbf{g}_n|^2 \right)^{1/2}, \quad (4)$$

we can write Eqn (2) briefly as

$$A = \mathbf{w}^* \bar{\mathbf{C}} \mathbf{w}, \quad (5)$$

where the asterisk now stands for complex conjugate transposition.

2.2 Point Spread Functions

Suppose there is a unit source in a scan point $\vec{\xi}_j$. This source induces a CSM by

$$\mathbf{C}_j = \mathbf{g}_j \mathbf{g}_j^*. \quad (6)$$

The CB method renders source powers A_{jk} in scan points $\vec{\xi}_k$ by

$$A_{jk} = \mathbf{w}_k^* \bar{\mathbf{C}}_j \mathbf{w}_k = \mathbf{w}_k^* \left[\overline{\mathbf{g}_j \mathbf{g}_j^*} \right] \mathbf{w}_k. \quad (7)$$

This expression is called the Point Spread Function (PSF). It describes the array response of a point source. By definition we have $A_{jk} = 1$ for $j = k$, and ideally we would have $A_{jk} = 0$, for $j \neq k$. However, with a finite number of microphones this is not possible. Array microphone layouts are usually designed such that A_{jk} , for $j \neq k$, is minimized in a certain frequency range.

2.3 Deconvolution using CLEAN-PSF

Assuming that a source plot is built up by PSF's, we can perform a deconvolution using the CLEAN⁹ algorithm. This is a technique that astronomical researchers use to remove side lobes of bright stars from maps obtained with multiple telescopes. Basically, CLEAN performs the following steps:

- Obtain a source plot by CB (“dirty map”).
- Search for the peak location in the dirty map.
- Subtract the appropriately scaled PSF from the dirty map.
- Replace this PSF by a “clean beam” (beam without side lobes).

This process is done iteratively, so that deconvolutions are made of multiple sources.

The iteration starts with iteration $i = 0$, for which we define the “degraded” CSM:

$$\mathbf{D}^{(i)} = \mathbf{D}^{(0)} = \mathbf{C}. \quad (8)$$

Using CB, source powers $P_j^{(0)}$ are calculated for points $\vec{\xi}_j$ on the scan grid:

$$P_j^{(0)} = \mathbf{w}_j^* \bar{\mathbf{C}} \mathbf{w}_j = \mathbf{w}_j^* \bar{\mathbf{D}}^{(0)} \mathbf{w}_j. \quad (9)$$

Herewith, a dirty map is created. For $i \geq 1$, the following analysis is made.

[\Rightarrow] In the dirty map, the peak source location $\vec{\xi}_{\max}^{(i)}$ is determined, i.e., the scan point $\vec{\xi}_j$ for which $P_j^{(i-1)}$ obtains its maximum value $P_{\max}^{(i-1)}$. The contribution of the source in $\vec{\xi}_{\max}^{(i)}$ has to be subtracted from the dirty map. Degraded source powers $P_j^{(i)}$ without the influence of this peak source, are formally written as

$$P_j^{(i)} = P_j^{(i-1)} - \mathbf{w}_j^* \bar{\mathbf{G}}^{(i)} \mathbf{w}_j, \quad (10)$$

where $\mathbf{G}^{(i)}$ is the CSM induced by the source in $\vec{\xi}_{\max}^{(i)}$. It is assumed that this matrix is given by

$$\mathbf{G}^{(i)} = P_{\max}^{(i-1)} \mathbf{g}_{\max}^{(i)} \mathbf{g}_{\max}^{*(i)}, \quad (11)$$

where $\mathbf{g}_{\max}^{(i)}$ is the steering vector associated with $\vec{\xi}_{\max}^{(i)}$. Eqn (10) can thus be written as

$$P_j^{(i)} = P_j^{(i-1)} - P_{\max}^{(i-1)} \mathbf{w}_j^* \left[\mathbf{g}_{\max}^{(i)} \mathbf{g}_{\max}^{*(i)} \right] \mathbf{w}_j. \quad (12)$$

In other words, the dirty map is updated by subtracting a scaled PSF associated with $\vec{\xi}_{\max}^{(i)}$. This PSF is replaced by a clean beam:

$$Q_j^{(i)} = P_{\max}^{(i-1)} \Phi \left(\vec{\xi}_j - \vec{\xi}_{\max}^{(i)} \right), \quad (13)$$

where Φ is a normalized clean beam of specified width, and maximum value $\Phi(0) = 1$. Finally, a degraded CSM is defined:

$$\mathbf{D}^{(i)} = \mathbf{D}^{(i-1)} - P_{\max}^{(i-1)} \mathbf{g}_{\max}^{(i)} \mathbf{g}_{\max}^{*(i)}, \quad (14)$$

so that we have, analogously to Eqn (9),



$$P_j^{(i)} = \mathbf{w}_j^* \bar{\mathbf{D}}^{(i)} \mathbf{w}_j. \quad (15)$$

Then, the next iteration can be made. [↩]

After I iterations, the source plot is written as a summation of the clean beams and the remaining dirty map:

$$A_j = \sum_{i=1}^I Q_j^{(i)} + P_j^{(I)}. \quad (16)$$

A good stop criterion is probably

$$\|\bar{\mathbf{D}}^{(I+1)}\| \geq \|\bar{\mathbf{D}}^{(I)}\|. \quad (17)$$

In other words, it makes sense to stop if the degraded CSM contains more “information” than in the previous iteration. A possible choice for the norm in Eqn (17) is

$$\|\bar{\mathbf{C}}\| = \sum_{(m,n) \in S} |C_{nm}|. \quad (18)$$

Often a safety factor φ (called “loop gain”), with $0 < \varphi \leq 1$, is used in the CLEAN algorithm. This means that Eqns (13) and (14) are replaced by

$$\begin{cases} Q_j^{(i)} = \varphi P_{\max}^{(i-1)} \Phi(\vec{\xi}_j - \vec{\xi}_{\max}^{(i)}), \\ \mathbf{D}^{(i)} = \mathbf{D}^{(i-1)} - \varphi P_{\max}^{(i-1)} \mathbf{g}_{\max}^{(i)} \mathbf{g}_{\max}^{*(i)}. \end{cases} \quad (19)$$

The CLEAN algorithm sketched here is based on the assumption that source plots are built up by PSF’s. Therefore, we will name this method “CLEAN-PSF.” It assumes that the sound field is described by a finite number of point sources, of which the sound transfer is described by the steering vector \mathbf{g} . This includes the assumption of uniform source directivity and no loss of coherence. These assumptions are seldom fulfilled in aero-acoustic measurements. Also, inaccuracies in microphone sensitivities may contaminate the source assumption. To overcome the limitations of CLEAN-PSF, an alternative is proposed hereafter.

2.4 Deconvolution using CLEAN-SC

To overcome the disadvantages of CLEAN-PSF, a method is proposed that makes use of the fact that side lobes in a source plot are coherent with the main lobe⁸. Use is made of source cross-powers, which are defined by

$$B_{jk} = \mathbf{w}_j^* \bar{\mathbf{C}} \mathbf{w}_k. \quad (20)$$

The degraded source powers $P_j^{(i)}$ are written as in Eqn (10), but now a different choice is made for the matrix $\mathbf{G}^{(i)}$. It is demanded that the source cross-powers of any scan point $\bar{\xi}_j^{(i)}$ with the peak location $\bar{\xi}_{\max}^{(i)}$ are determined entirely by $\mathbf{G}^{(i)}$. In other words,

$$\mathbf{w}_j^* \bar{\mathbf{D}}^{(i-1)} \mathbf{w}_{\max}^{(i)} = \mathbf{w}_j^* \bar{\mathbf{G}}^{(i)} \mathbf{w}_{\max}^{(i)}, \text{ for all possible } \mathbf{w}_j, \quad (21)$$

where $\mathbf{w}_{\max}^{(i)}$ is the weight vector associated with $\mathbf{g}_{\max}^{(i)}$. Equation (21) is satisfied when

$$\bar{\mathbf{D}}^{(i-1)} \mathbf{w}_{\max}^{(i)} = \bar{\mathbf{G}}^{(i)} \mathbf{w}_{\max}^{(i)}. \quad (22)$$

Equation (22) does not have a unique solution for $\mathbf{G}^{(i)}$, but we can construct one when we assume that $\mathbf{G}^{(i)}$ is due to a single coherent source component $\mathbf{h}^{(i)}$:

$$\mathbf{G}^{(i)} = P_{\max}^{(i-1)} \mathbf{h}^{(i)} \mathbf{h}^{*(i)}, \quad (23)$$

For the trimmed version of Eqn (23) we write

$$\bar{\mathbf{G}}^{(i)} = P_{\max}^{(i-1)} \overline{\mathbf{h}^{(i)} \mathbf{h}^{*(i)}} = P_{\max}^{(i-1)} (\mathbf{h}^{(i)} \mathbf{h}^{*(i)} - \mathbf{H}^{(i)}), \quad (24)$$

where $\mathbf{H}^{(i)}$ is given by

$$H_{mn}^{(i)} = \begin{cases} 0, & \text{for } (m, n) \in S, \\ h_m^{(i)} h_n^{*(i)}, & \text{for } (m, n) \notin S. \end{cases} \quad (25)$$

Eqn (22) is solved when

$$\mathbf{h}^{(i)} = \frac{1}{\left(1 + \mathbf{w}_{\max}^{*(i)} \mathbf{H}^{(i)} \mathbf{w}_{\max}^{(i)}\right)^{1/2}} \left(\frac{\bar{\mathbf{D}}^{(i-1)} \mathbf{w}_{\max}^{(i)}}{P_{\max}^{(i-1)}} + \mathbf{H}^{(i)} \mathbf{w}_{\max}^{(i)} \right). \quad (26)$$

This is not an explicit expression for $\mathbf{h}^{(i)}$, as $\mathbf{H}^{(i)}$ contains (the diagonal) elements of $\mathbf{h}^{(i)} \mathbf{h}^{*(i)}$. However, we can work out Eqn (26) iteratively, starting with $\mathbf{h}^{(i)} = \mathbf{g}_{\max}^{(i)}$. Usually, only a few iterations are required for convergence.

With Eqn (23), we have an alternative expression for Eqn (11), which does not make use of the transfer vectors $\mathbf{g}_{\max}^{(i)}$, except to define the weight vector $\mathbf{w}_{\max}^{(i)}$. Starting from this expression for $\mathbf{G}^{(i)}$, we can further perform the same CLEAN algorithm as in the previous section. This alternative CLEAN method is called ‘‘CLEAN based on spatial Source Coherence’’ or, briefly, ‘‘CLEAN-SC.’’ Analogously to Eqn (19), the iterations of CLEAN-SC can be summarized by

$$\begin{cases} Q_j^{(i)} = \varphi P_{\max}^{(i-1)} \Phi(\vec{\xi}_j - \vec{\xi}_{\max}^{(i)}), \\ \mathbf{D}^{(i)} = \mathbf{D}^{(i-1)} - \varphi P_{\max}^{(i-1)} \mathbf{h}^{(i)} \mathbf{h}^{*(i)}. \end{cases} \quad (27)$$

2.5 Determination of absolute source contributions using CLEAN-SC

After I iterations, the original CSM can be written as

$$\mathbf{C} = \varphi \sum_{i=1}^I P_{\max}^{(i-1)} \mathbf{h}^{(i)} \mathbf{h}^{*(i)} + \mathbf{D}^{(I)}. \quad (28)$$

If the CSM is sufficiently degraded, i.e., if $\|\bar{\mathbf{D}}^{(I)}\| \ll \|\bar{\mathbf{C}}\|$, then the first term in the right hand side of Eqn (28) contains the essential information of the most important sources in the scan plane, and the second term is dominated by noise, especially for matrix components with $(m, n) \notin S$. In other words, the signal part of the CSM can be approximated by

$$\mathbf{C}_{\text{signal}} = \varphi \sum_{i=1}^I P_{\max}^{(i-1)} \mathbf{h}^{(i)} \mathbf{h}^{*(i)}. \quad (29)$$

Herewith, we have a tool for reconstructing the signal-induced cross-spectra for $(m, n) \notin S$.

This is especially interesting when the diagonal was removed from the CSM, due to high noise levels in the auto-spectra (e.g., boundary layer noise in closed wind tunnel sections). Using Eqn (29), the CSM diagonal can be reconstructed, in other words, the auto-spectra due to the relevant sources can be calculated. The summed microphone auto-spectra (trace of the CSM) can be written as

$$\sum_{n=1}^N C_{nn} = \varphi \sum_{i=1}^I P_{\max}^{(i-1)} \sum_{n=1}^N h_n^{(i)} h_n^{*(i)} = \varphi \sum_{i=1}^I P_{\max}^{(i-1)} \|\mathbf{h}^{(i)}\|^2. \quad (30)$$

Thus, a breakdown into absolute contributions from source components is made.

3 Application to wind tunnel measurements

3.1 Typical results

CLEAN-SC was tested on array measurements of an Airbus A340 1:10.6 scale model in the 8×6 m² closed test section of DNW-LLF. These tests were carried out within the EU-project AWIATOR, in which novel high lift devices were investigated. Measurements were done with a wall-mounted array of 128 microphones, underneath the starboard wing. For a typical configuration at 60 m/s wind speed, source plots obtained with CB (with diagonal removal) are

shown in Fig. 1. The results are shown in dB relative to the peak value. The map size is 2.5×3.0 m² and the grid spacing is 2.5 cm.

The same measurements were also processed with CLEAN-SC, the results of which are shown in Fig. 2. For the loop gain in the iteration process we chose $\varphi = 0.99$. For the entire range of frequencies, the widths of the clean beams were set to 5 cm at 3 dB below the peak. Up to 2500 Hz, the clean beam positions are a bit arbitrary, as CLEAN-SC just bunches together extended coherent source regions into single points: the peak locations. However, a number of sources are revealed that are not visible in Fig. 2. At higher frequencies the clean beams seem to be correctly located, and a significant improvement in spatial resolution is observed. At the leading edge, regularly spaced sources can be observed, which coincide with the slat tracks. The number of iterations (I) varied with frequency, as shown in Fig. 3.

CLEAN-SC was also used for integrated source power determination (see Sec. 2.2.5). A summation was made of the (appropriately scaled) source components (Eqn (30)), and the results of conventional Source Power Integration¹⁰ (SPI) applied to the degraded CSM $\mathbf{D}^{(I)}$ was added. The results are shown in Fig. 4, where a comparison is made with SPI applied to the original CSM \mathbf{C} . The results of CLEAN-SC and conventional SPI agree very well, which is remarkable, since the algorithms are completely different.

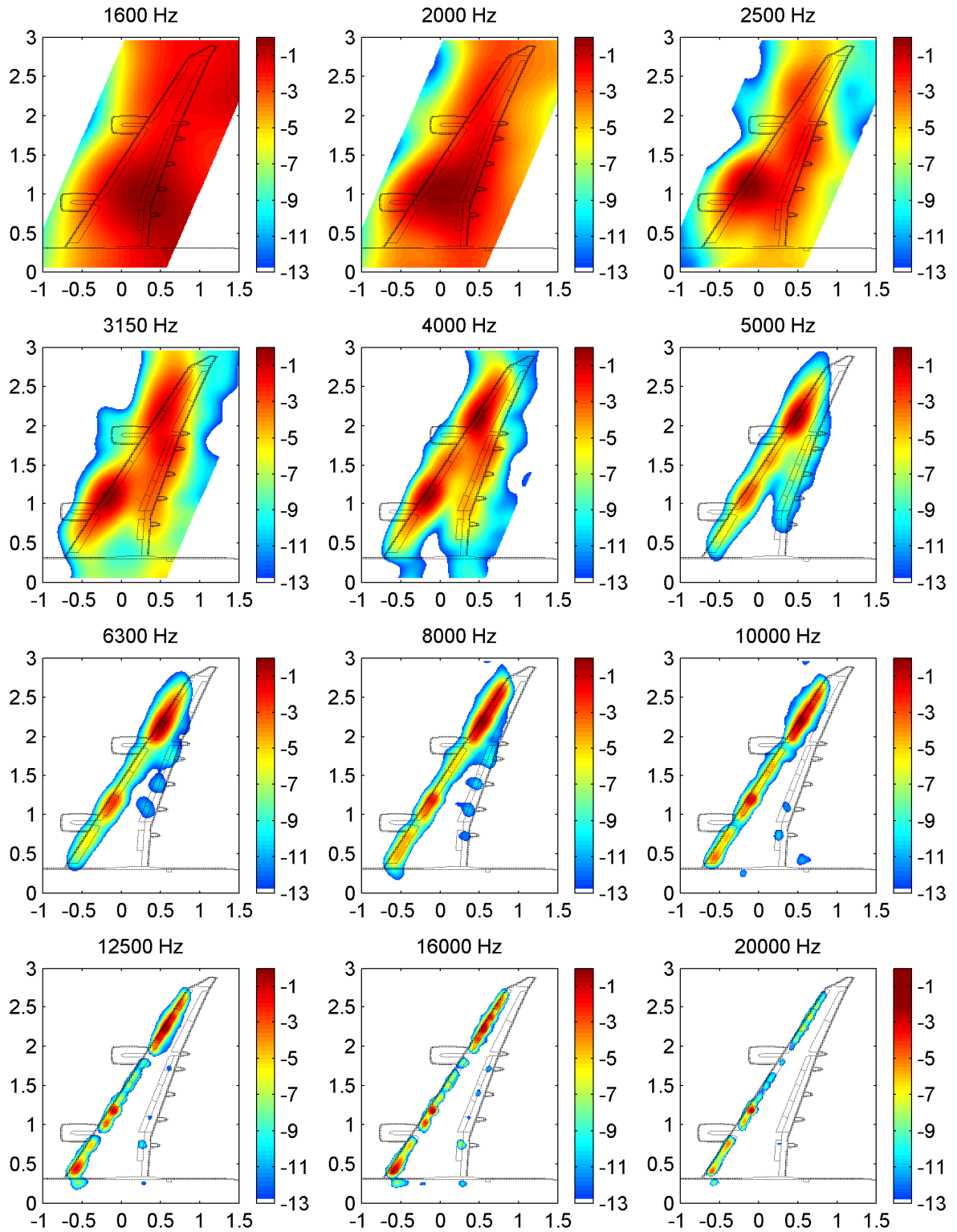


Figure 1: Typical CB results of A340 scale model at 60 m/s wind speed, range = 13 dB.

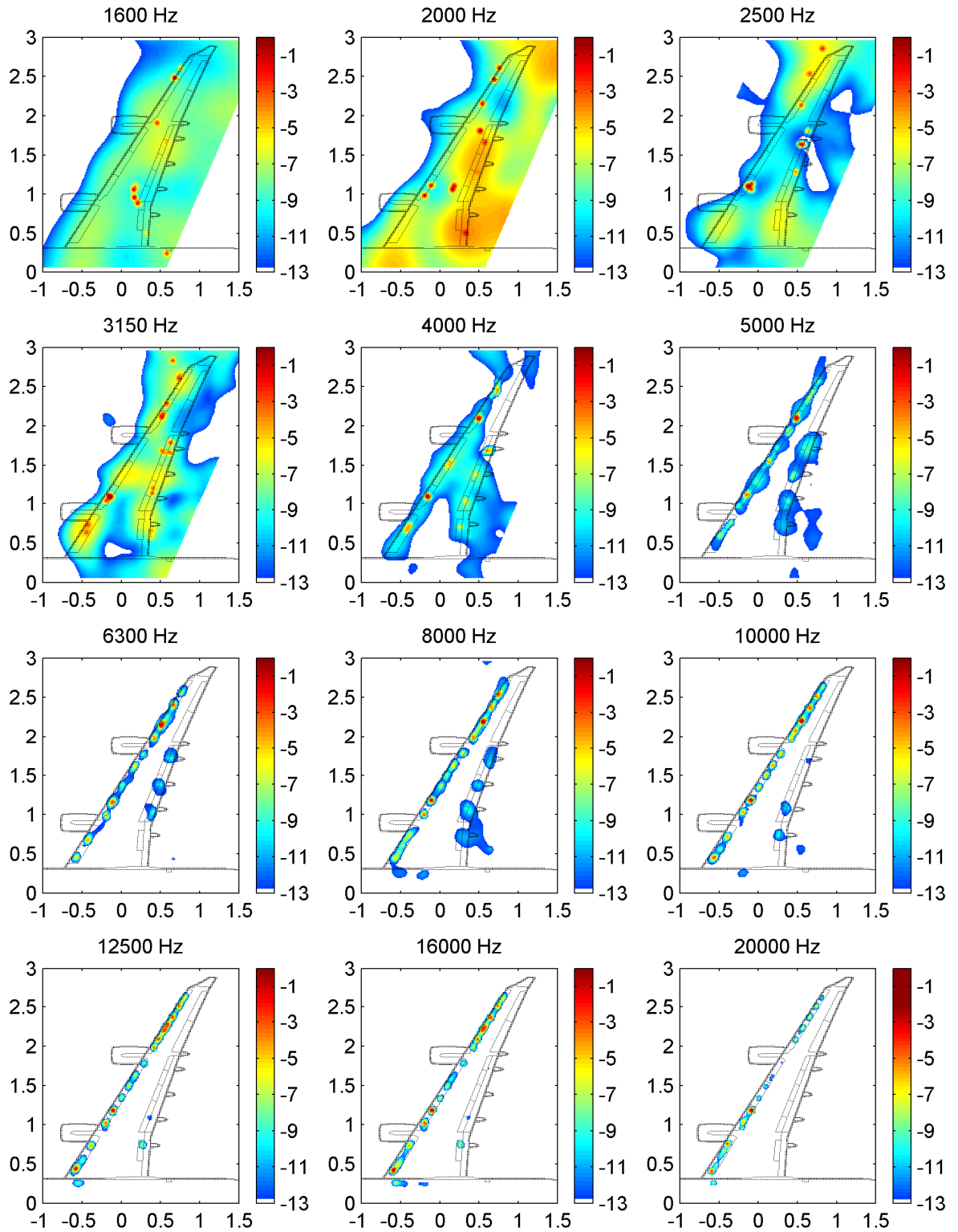


Figure 2: Same test data as Fig. 1, processed with CLEAN-SC.

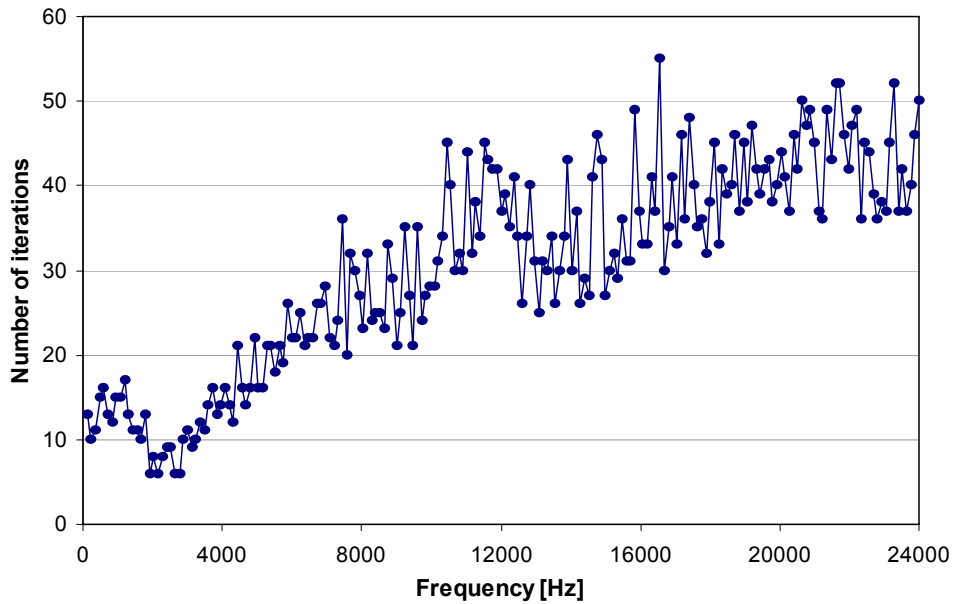


Figure 3: Number of iterations of CLEAN-SC.

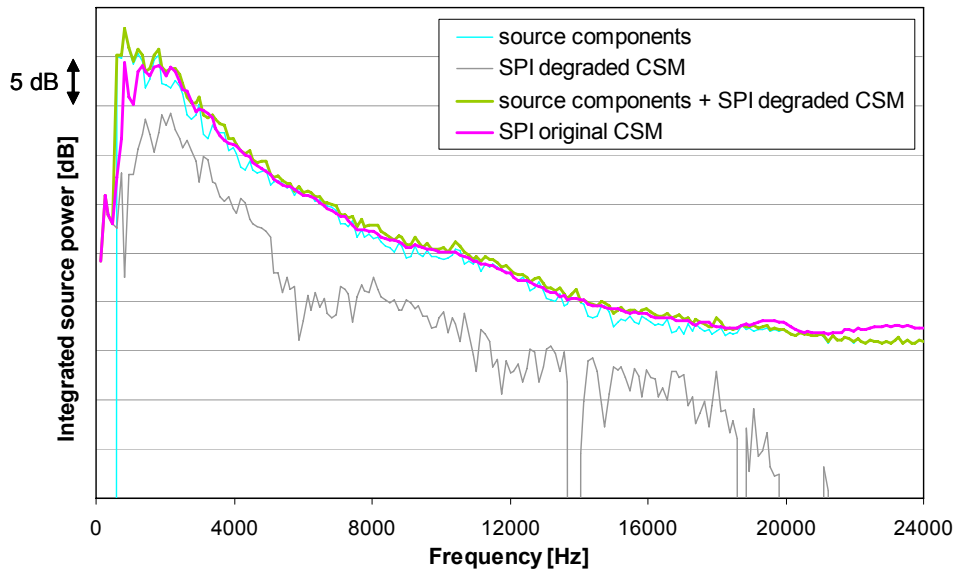


Figure 4: Source power spectra.

3.2 Removal of dominant sources

CLEAN-SC is a very suitable tool for the elimination of dominant sources. We will illustrate this using another configuration from the same A340 closed test section wind tunnel measurements. For this configuration, at a few frequency lines, a strong source appeared at the outer-wing slat. An example of a CB source plot at such a frequency line is shown in Fig. 5. The plot range in this figure is 13 dB, which is about the same as the dynamic range (peak level minus highest side lobe level) of the array that was used.

This outer-wing slat noise source was not representative for a full-scale A340. In fact, the source was due to low Reynolds number flow, and could be removed by applying zigzag tape for fixation of the turbulence transition. Secondary sources, on other parts of the leading edge, are more interesting. But these are not visible in Fig. 5, because their levels are more than 13 dB below the peak source. Increasing the plot range to 31 dB, as in Fig. 6, does not provide useful additional information. There may be sources visible at the leading edge, but they can not be distinguished from spurious sources outside the wing, which are apparently side lobes of the main source. By removing the main source from Fig. 6, including all the side lobes, more insight would be gained into the location and strength of the secondary sources.

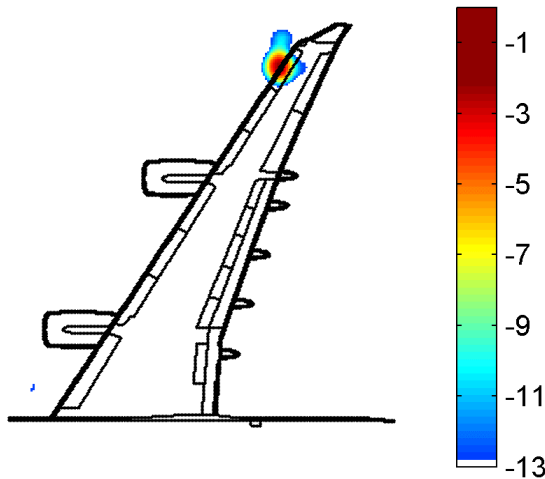


Figure 5: Source plot at 12360 Hz, CB, range = 13 dB.

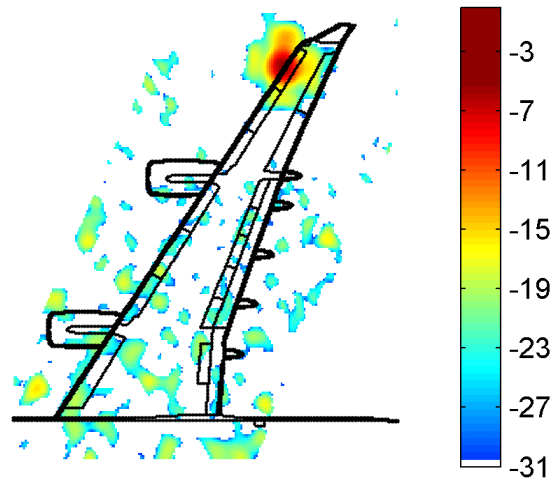


Figure 6: Source plot at 12360 Hz, CB, range = 31 dB.

In Ref. 11, it was proposed to consider the eigenvalue decomposition of \mathbf{C} , and remove the eigenvector corresponding to the highest eigenvalue, i.e., the first principal component (PC). This idea was applied to the trimmed CSM of the current test data, the result of which is shown in Fig. 7. The peak in this plot is 18 dB lower than in Fig. 5, and sources on the leading edge can now be recognized well. A disadvantage of this method is that the first PC may contain more information than just the main source. Moreover, the application of PC analysis to a trimmed CSM is hazardous, because such a matrix is not positive-definite.

A different way to unmask secondary sources is removing the scaled PSF from the source plot. The result, which is shown in Fig. 8, is disappointing, because there are still remainders visible of the main source and its side lobes. In contrast with the PC removal method, real sources can not be distinguished from side lobes. Apparently, the theoretical PSF does not have the same shape as the actual beam pattern of the main source. In other words, the microphone pressures induced by the main source are not proportional to the steering vector \mathbf{g}_{\max} .

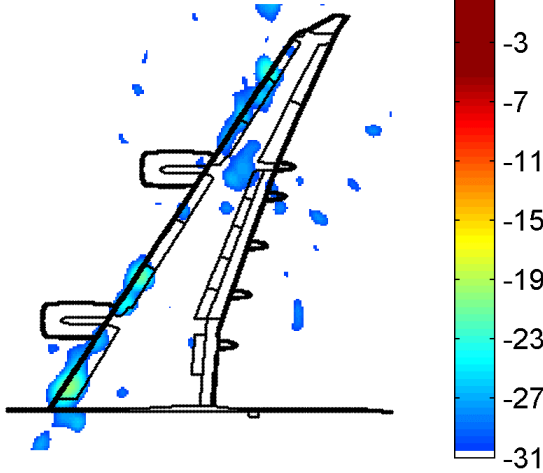


Figure 7: Source plot at 12360 Hz, CB, after PC removal, peak at -17.6 dB.

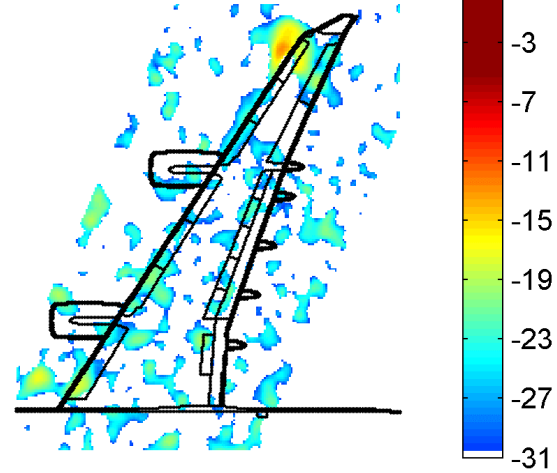


Figure 8: Source plot at 12360 Hz, CB, after PSF removal, peak at -9.3 dB.

Main source removal using the PSF is, in fact, the first iteration of CLEAN-PSF, where the CSM \mathbf{C} is replaced by $\mathbf{C} - P_{\max}^{(0)} \mathbf{g}_{\max}^{(1)} \mathbf{g}_{\max}^{*(1)}$ (with loop gain $\varphi = 1$). We can also use the first iteration of CLEAN-SC, i.e. replace \mathbf{C} by $\mathbf{C} - P_{\max}^{(0)} \mathbf{h}^{(1)} \mathbf{h}^{*(1)}$. The result is shown in Fig. 9, where the actual leading-edge sources can now be recognized well. Compared to the PC removal results of Fig. 7, more sources are visible, and the levels are higher. This indicates that the PC removal method may indeed remove too much information. Note that Figs. 7 to 9 reveal leading edge sources, between the main source and the outer engine, which are not visible (i.e., below the threshold) in Fig. 6. The reason for this invisibility is that CB with diagonal removal provides negative side lobes of the main source in that region, thus “pushing away” the secondary sources.

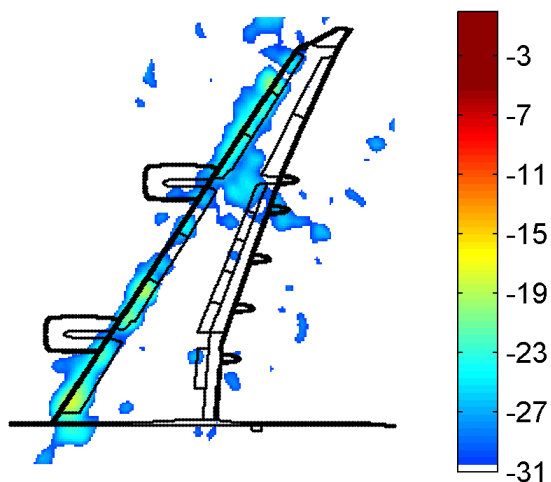


Figure 9: Source plot at 12360 Hz, CB, after coherent source removal, peak at -15.5 dB.

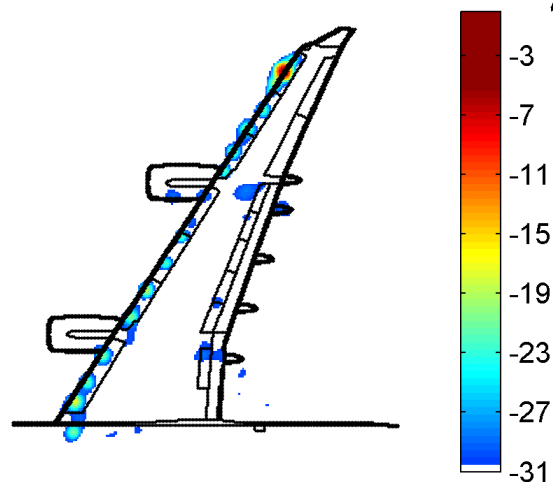


Figure 10: Source plot at 12360 Hz, CLEAN-SC.

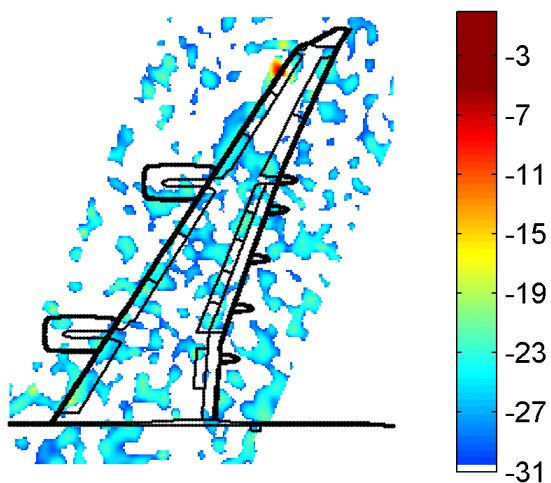


Figure 11: Source plot at 12360 Hz, CLEAN-PSF.

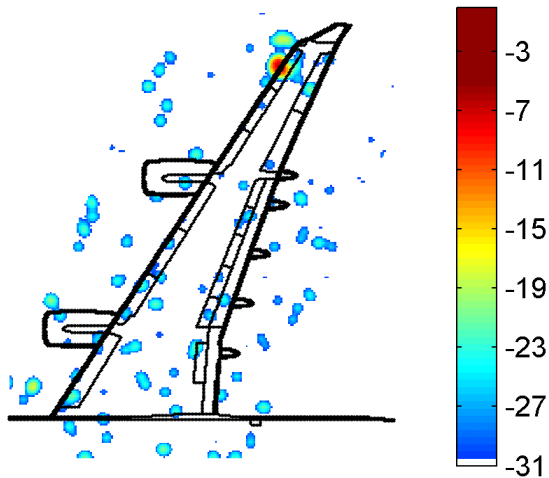


Figure 12: Source plot at 12360 Hz, DAMAS.

4 Remarks about CLEAN-SC

4.1 Processing speed

For standard wind tunnel microphone array applications, where beamforming methods are applied to the CSM without the diagonal, there is relatively short time needed to run CLEAN-SC. Only for iteration $i=0$, which is equivalent to CB, a double summation, Eqn (9), is required. For the other iterations, we can write

$$P_j^{(i)} = P_j^{(i-1)} - P_{\max}^{(i-1)} \mathbf{w}_j^* \left[\mathbf{h}^{(i)} \mathbf{h}^{*(i)} \right] \mathbf{w}_j = P_j^{(i-1)} - P_{\max}^{(i-1)} \left(\left| \sum_{n=1}^N w_{j,n}^* h_n^{(i)} \right|^2 - \sum_{n=1}^N |w_{j,n}^* h_n^{(i)}|^2 \right). \quad (31)$$

Equation (31) shows that dirty maps can be updated by evaluating single summations, which is done much faster than double summations. In practice, the total processing time for CLEAN-SC is about twice as long as for CB.

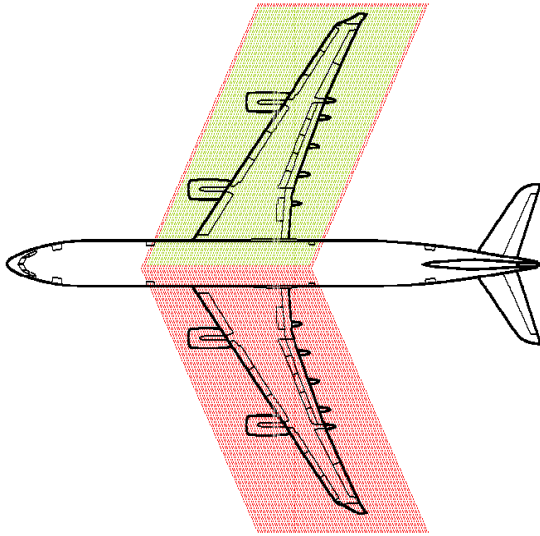


Figure 13: Scan grid used for Fig. 4.

4.2 Sources outside the scan area

After removal of a number of sound sources from the dirty map, it may be possible that the next peak value corresponds to a side lobe of a source outside the scan area. However, the corresponding source component in the auto-spectrum (see Eqn (30)) will then be due to the actual, external source, thus giving a wrong contribution to the total source power from the scan area. Therefore, it is better to use a larger grid, containing all the expected sound source locations. When a peak source is found outside the area of interest, its source component can be excluded from the summation of Eqn (30). For the integrated spectra shown in Fig. 4, we used the scan grid shown in Fig. 13, where peak sources in the red area were rejected.

4.3 Reflected sources

Reflections of acoustic sources, e.g., due to a wind tunnel wall, are (in principle) coherent with the primary source, and may thus give an erroneous contribution to the calculated source levels. In the example shown here (DNW-LLF), this was not a real problem. The reflected sources appeared to be incoherent with the actual source (maybe because of different emission angles). Reflections can become a more serious issue in smaller wind tunnels, where the sound sources are closer to the walls.

4.4 Closely spaced sources

It is noted that the CLEAN approach is fundamentally different from deconvolution methods that basically solve a system of equations, like DAMAS. CLEAN-SC makes the simplifying assumption that peaks in source plots are due to single sources. But if two sources are closely spaced, such that their main lobes significantly interfere, then CLEAN-SC will not be able to separate them correctly. The summed level will be correct, however.

4.5 Noise

The source components obtained with CLEAN-SC may contain (boundary layer) noise which is still present in $\bar{\mathbf{C}}$, i.e., in the cross-spectra. The source components contain relatively more noise than the source powers obtained with CB. Therefore, the SPI curve (obtained from the original CSM) in Fig. 4 is smoother than the CLEAN-SC curves. CLEAN-SC will probably benefit from long acquisition times, because that will reduce the noise in the cross-spectra.

4.6 CLEAN-SC using full CSM

When the full CSM is used for beamforming, i.e., when $\bar{\mathbf{C}} = \mathbf{C}$, then for Eqn (26) we have

$$\mathbf{h}^{(i)} = \frac{\mathbf{D}^{(i-1)} \mathbf{w}_{\max}^{(i)}}{P_{\max}^{(i-1)}}. \quad (32)$$

Consequently, the degraded source powers can be rewritten as

$$\begin{aligned} P_j^{(i)} &= P_j^{(i-1)} - \mathbf{w}_j^* \mathbf{G}^{(i)} \mathbf{w}_j = P_j^{(i-1)} - P_{\max}^{(i-1)} \mathbf{w}_j^* \mathbf{h}^{(i)} \mathbf{h}^{*(i)} \mathbf{w}_j = P_j^{(i-1)} - P_{\max}^{(i-1)} \mathbf{w}_j^* \frac{\mathbf{D}^{(i-1)} \mathbf{w}_{\max}^{(i)}}{P_{\max}^{(i-1)}} \frac{\mathbf{w}_{\max}^{*(i)} \mathbf{D}^{(i-1)}}{P_{\max}^{(i-1)}} \mathbf{w}_j \\ &= P_j^{(i-1)} \left[1 - \frac{|\mathbf{w}_j^* \mathbf{D}^{(i-1)} \mathbf{w}_{\max}^{(i)}|^2}{P_j^{(i-1)} P_{\max}^{(i-1)}} \right] = P_j^{(i-1)} \left[1 - \frac{|\mathbf{w}_j^* \mathbf{D}^{(i-1)} \mathbf{w}_{\max}^{(i)}|^2}{(\mathbf{w}_j^* \mathbf{D}^{(i-1)} \mathbf{w}_j) (\mathbf{w}_{\max}^* \mathbf{D}^{(i-1)} \mathbf{w}_{\max}^{(i)})} \right]. \end{aligned} \quad (33)$$

This is briefly written as

$$P_j^{(i)} = P_j^{(i-1)} \left[1 - \gamma_{j,\max}^{2(i)} \right], \quad (34)$$

where $\gamma_{j,\max}^{2(i)}$ is the spatial coherence in the dirty map, between $\vec{\xi}_j$ and $\vec{\xi}_{\max}^{(i)}$. An analogous expression can not be derived when beamforming is done without the full CSM.

5 Conclusion

A new deconvolution method for acoustic array measurements is proposed: CLEAN-SC. This is an alternative version, based on spatial source coherence, of the classical CLEAN algorithm. Compared with other deconvolution methods, better results can be obtained, because CLEAN-SC does not assume a theoretical beam pattern (PSF). The merits were demonstrated using airframe noise measurements on a scale model of the Airbus A340. It was found that CLEAN-SC is a very effective tool to remove dominant sources from source plots, thereby unmasking secondary sources. Like other deconvolution algorithms, significant improvements in spatial resolution were found. Moreover, CLEAN-SC is able to extract absolute values of source components from the source plots. Summed results of these source powers agree very well with results of the conventional SPI technique. The processing time of CLEAN-SC is relatively short: about twice as long as for CB.

Acknowledgment

CLEAN-SC was tested on wind tunnel measurements in the 8×6 m² closed test section of DNW-LLF, performed within the EU-project AWIATOR (6th Framework).

References

1. Blacodon, D., and Elias, G., "Level Estimation of Extended Acoustic Sources using a Parametric Method", Journal of Aircraft, November-December 2004, Vol. 41 (No. 6), pp. 1360-1369.
2. Brooks, T.F., and Humphreys, W.M., "A Deconvolution Approach for the Mapping of Acoustic Sources (DAMAS) Determined from Phased Microphone Arrays", Journal of Sound and Vibration, March 2006, Vol. 294, pp. 856-879 (also AIAA Paper 2004-2954, May 2004).
3. Brooks, T.F., and Humphreys, W.M., "Three-Dimensional Application of DAMAS Methodology for Aeroacoustic Noise Source Definition", AIAA Paper 2005-2960, May 2005.
4. Dougherty, R.P., "Extensions of DAMAS and Benefits and Limitations of Deconvolution in Beamforming", AIAA Paper 2005-2961, May 2005.
5. Brooks, T.F., and Humphreys, W.M., "Extension of DAMAS Phased Array Processing for Spatial Coherence Determination (DAMAS-C)", AIAA Paper 2006-2654, May 2006.

6. Ravetta, P., Burdisso, R., and Ng, W., "Noise Source Localization and Optimization of Phased Array Results (LORE)", AIAA Paper 2006-2713, May 2006.
7. Ehrenfried, K., and Koop, L., "A Comparison of Iterative Deconvolution Algorithms for the Mapping of Acoustic Sources", AIAA Paper 2006-2711, 2006.
8. Oerlemans, S., and Sijtsma, P., "Determination of Absolute Levels from Phased Array Measurements using Spatial Coherence", AIAA Paper 2002-2464, June 2002.
9. Högbom, J.A., "Aperture Synthesis with a Non-Regular Distribution of Interferometer Baselines", Astron. Astrophys. Suppl., 1974, No. 15, pp. 417-426.
10. Brooks, T.F., and Humphreys, W.M., "Effect of Directional Array Size on the Measurement of Airframe Noise Components", AIAA Paper 99-1958, May 1999.
11. Dougherty, R.P., "Source Location with Sparse Acoustic Arrays; Interference Cancellation", Presented at the First CEAS-ASC Workshop: Wind Tunnel Testing in Aeroacoustics, DNW, 5-6 November 1997.
12. Dougherty, R.P., and Stoker, R.W., "Sidelobe Suppression for Phased Array Aeroacoustic Measurements", AIAA Paper 98-2242, June 1998.